Journal of
Translational Regenerative Medicine

2026. Volume 1

Research Paper

Genetic and Epigenetic Analysis of Zinc Oxide Nanoparticles on Autophagy Related Long Non-coding in Breast Cancer

Ali Saberian[1], Mostafa Akbariqomi[2*], Sara Keshtkari[3, 4], Reza Heidari[4]

1. Department of Food Science and Technology, SHK.C., Islamic Azad University, Shahrekord, Iran.
2. Applied Biotechnology Research Centre, Baqiyatallah University of Medical Sciences, Tehran, Iran.
3. Infectious Diseases Research Center, Aja University of Medical Sciences, Tehran, Iran.
4. Department of Internal Medicine, Aja University of Medical Sciences, Tehran, Iran.
5. Medical Biotechnology Research Center, AJA University of Medical Sciences, Tehran, Iran.

Use your device to scan and read the article online

Citation Saberian A, Akbariqomi M, Keshtkari S, Heidari R. Genetic and Epigenetic Analysis of Zinc Oxide Nanoparticles on Autophagy Related Long Non-coding in Breast Cancer. Journal of Translational Regenerative Medicine. 2025; 1:E1012. http://dx.doi.org/10.32598/JTRM.1.1012

http://dx.doi.org/10.32598/JTRM.1.1012

ABSTRACT

Background: Zinc-oxide (ZnO) nanoparticles (NPs) have wide industrial and biomedical applications. Determining the mechanisms of NPs action is challenging in clinical application particularly in future cancer therapy. However, the genetic and epigenetics effect of ZnO-NPs on autophagy (ATG) and apoptosis related long non-coding RNA (lncRNA) have not been studied.

Methods: ZnO-NPs were synthesized, characterized, and evaluated their effects on MCF-7 cells. In the following, breast cancer cells were treated with ZnO-NPs in the presence or absence of N-acetyl-L-cysteine (NAC, reactive oxygen species [ROS] inhibitor), 3-methyladenine (3-MA, ATG inhibitor), and Z-VAD-FMK (apoptosis inhibitor). Finally, genetic and epigenetic modification on ATG and apoptosis related lncRNA, such as DNA methylation, histones modification, and alteration in lncRNA expression were investigated.

Results: Comparison between non-exposed and exposed cells revealed a significant increase in GAS5 expression, whereas XIST, TUG1, and MALAT1 were significantly downregulated. Histone modification analysis demonstrated enrichment of H3K4me3 at the GAS5 promoter. In contrast, H3K27me3 levels were significantly increased at the promoters of XIST, TUG1, and MALAT1. Consistently, promoter methylation analysis showed decreased methylation in GAS5, while methylation levels were significantly increased in XIST, TUG1, and MALAT1.

Conclusion: It seems that lncRNA modulate the crosstalk between ATG and apoptosis via regulating the expression of related genes. The present study may provide new insights into the mechanism of NPs interference with ATG and apoptosis related lncRNA in cancer therapeutic.

Keywords: Zinc-oxide nanoparticles (ZnO-NPs), Breast cancer, Long non-coding RNA (lncRNA), Epigenetic modification, Reactive oxygen species (ROS), Autophagy (ATG), Apoptosis

Article info:
Received: 10 Feb 2026
Accepted: 23 Apr 2026
Publish: 13 Jun 2026

*** Corresponding Author:**
Mostafa Akbariqomi, Associate Professor.
Address: *Applied Biotechnology Research Centre, Baqiyatallah University of Medical Sciences, Tehran, Iran.*
E-mail: *Mostafa.akbari63@yahoo.com*

Highlights

- ZnO nanoparticles altered the expression of key autophagy/apoptosis-related lncRNAs in MCF-7 breast cancer cells, including GAS5, XIST, TUG1, and MALAT1.

- ZnO-NPs induced epigenetic changes, with increased H3K4me3 and reduced methylation at the GAS5 promoter, and elevated H3K27me3 and methylation at XIST, TUG1, and MALAT1 promoters.

- The findings suggest that lncRNAs may mediate the crosstalk between autophagy and apoptosis in breast cancer cells exposed to ZnO nanoparticles.

Plain Language Summary

Breast cancer remains one of the most common cancers worldwide, and researchers are constantly exploring new ways to better understand how cancer cells grow and respond to treatment. In recent years, very small materials known as nanoparticles (NPs) have attracted attention in medical research because they may influence how cancer cells behave. Among these materials, zinc oxide nanoparticles (ZnO-NPs) have been widely studied for their potential biological and therapeutic effects. In this study, we investigated how zinc oxide nanoparticles affect breast cancer cells in the laboratory. Specifically, we examined whether these particles influence certain cellular processes that determine whether a cell survives or dies. Two of these processes are autophagy, which is a natural recycling system that helps cells cope with stress, and apoptosis, a programmed form of cell death that removes damaged or unwanted cells. We also focused on a group of molecules called long non-coding RNA (lncRNA). Although these molecules do not produce proteins, they play important roles in regulating gene expression. Our results showed that exposure to zinc oxide nanoparticles changed the activity of several important lncRNA, including *GAS5*, *XIST*, *TUG1*, and *MALAT1*. We also found that the nanoparticles induced chemical changes around these genes, which can influence whether they become more or less active. These changes suggest that nanoparticles may affect how cancer cells manage stress and balance survival and death pathways. Understanding how nanoparticles interact with cancer cells is important for both medicine and public health. These findings provide new insight into how nanomaterials may influence gene regulation in cancer cells. In the future, this knowledge may help researchers design safer nanomaterials and explore new strategies for cancer treatment and drug delivery.

Introduction

In recent years, nanomaterials have been at the center of attention of many researchers due to their unique and wonderful cancer applications, such as cancer detection, anticancer drug delivery, anticancer agents, anti-inflammatory activities and cancer therapeutic [1, 2]. Several studies have reported various effect of the nanoparticles (NPs) on DNA damages, inflammatory response, apoptosis, oxidative stress, immunotoxicity, reproductive toxicity and epigenetic mechanisms on both normal and cancer cells [3-5].

Zinc-oxide (ZnO) NPs with different sizes, surface charge, shapes, and morphology showed an oxidative stress and genotoxic effect [6]. ZnO-NPs have exhibited a high degree of selective cytotoxicity and anticancer performance towards the cancer cells [7, 8]. Several studies show that ZnO-NPs a promising new class of anticancer agents [8, 9]. Also, ZnO-NPs has the potential to alter cellular metabolism, genetic and epigenetic patterns, such as aberrant DNA methylation, non-coding RNA (ncRNA) expression and histone modification [10-12]. The most important mechanisms of ZnO-NPs on cancer cell include increasing levels of cellular reactive oxygen species (ROS) and subsequent induce intrinsic apoptosis and autophagy (ATG) [9, 13, 14].

ATG and apoptosis are highly conserved pathway and regulated cellular process, which is crucial for response to metabolic stress [15]. The targets of ATG include degraded and recycled proteins and organelles under stressful conditions [16]. In breast cancer cells, core proteins can be identified for regulated apoptosis (caspase-3, caspase-9, *Bax/Bcl-2*), and ATG (LC3II/LC3I ratio, *Atg5*, *Beclin-1*) [17]. Recently studies have shown that ZnO-NPs can induce ATG and apoptosis in several cells and

tissues [18-20]. The results of recent study show that ncRNA generally control ATG and apoptosis via regulating the expression of related genes [21, 22].

ncRNA is a powerful tool for controlling the vital function of cells by interacting with macro-molecules [23]. Long ncRNA (lncRNAs) are longer than 200 nucleotides with ability encoding peptide (<100 amino acids) or proteins as promising candidates in biomarkers and antitumor drugs [24]. Similar to pre-mRNA, lncRNAs are mainly transcribed by RNA polymerase II but in contrast, expression and conservation in exons are fewer in the lncRNA [23]. lncRNAs are involved in many critical aspects of cell function, such as epigenetic regulation, gene expression regulation metabolism, cell cycle, apoptosis, ATG and RNA splicing [25]. The aberrant lncRNAs expression has been detected in physiological and pathological conditions in various cancers, especially breast cancer occurrence, progression and development [23, 26]. Recent studies identified several lncRNAs in tight connection with breast cancer [23, 27, 28]. A common property of cancer cells is their ability to overcome environmental stresses. lncRNA acts as major regulator of cellular and environmental stress in cancer [29]. In other words, lncRNAs can sensitize and resist cells to response to drug and oxidative stress.

The first aim of this study was to provide evidence that ZnO-NPs could induce ATG in breast cancer. The second aim of the present study was to determine lncRNAs associated with ZnO-induced ATG and apoptosis in breast cancer cells. Finally, we evaluated genetic and epigenetic alteration in ATG and apoptosis related lncRNA in breast cancer cell. Our results will provide fundamental role of lncRNA in the mechanism of cellular response to oxidative stress and drug in breast cancer.

Materials and Methods

Study chemicals

Dulbecco's modified eagle's medium (DMEM), penicillin–streptomycin and fetal bovine serum were purchased from Life Technologies (Waltham, MA, USA) Invitrogen (Carlsbad, CA, USA). Then, (4,5-dimethylthiazol-2-yl)-2,5-diphenyltetrazolium bromide (MTT, M5655) hydrocortisone was purchased from Sigma-Aldrich (India). Also, 0.25% trypsin–ethylenediaminetetraacetic acid was purchased from Corning Incorporated (Corning, NY, USA). Insulin and horse serum were purchased from Gibco (Grand Island, NY, USA).

Synthesis of ZnO-NPs

The ZnO-NPs have been synthesized through the modified solvothermal method [30]. During this procedure, two solutions were prepared. For the solution A, 2.86 g Zn $(CH_3COO)_2.2H_2O$ was dissolved in 63 mL ethanol (99%) and was heated to 60 ˚C while stirring. Solution B, which contains KOH (0.75 g) and 35 mL ethanol (99%) is a precursor solution to the growth of ZnO-NPs. After the complete dissolve of chemicals in ethanol, solution B added dropwise to solution A stirring 100 rpm at 60 ˚C. In the next step, the final mixture was kept in room temperature for an hour. The solution was poured in a stainless-steel vessel (autoclave) and placed in a furnace at 150 ˚C for 18 h. After cooling down the sample to room temperature, the formed white precipitates were collected by centrifuging at 4000 rpm for 10 min. To remove the impurities, the collected white precipitates were washed with acetone and pure deionized water three times. Subsequently, the white precipitates were dried using the freeze drier overnight. The obtained dried product was ground two powder for later applications.

Database search and lncRNA signature selection

Selection, expression evaluation, and DNA methylation status of lncRNA consist of 4 phases.

Screening phase (I) is to select ATG/apoptosis related lncRNA for investigation in breast cancer according to the following items. We manually searched and retrieved paper list for additional studies and review articles. The inclusion criteria were as follows: ATG/apoptosis related lncRNA in human cancer analyzed using RNA analysis methods, such as quantitative PCR, RNA sequencing and microarrays; published between August 1, 2013 to June 30, 2022 as original and review articles without language restriction; and selective ATG/apoptosis related lncRNA expressed in breast cancer cells. The exclusion criteria were as follows: animal studies or the articles that could not be found in full.

Training phase (II) included downloading the differentially expressed genes in 1048 breast cancer sample from The Cancer Genome Atlas (TCGA) using cBioPortal. Top 12 significantly differentially expressed lncRNAs in breast cancer from both apoptosis and ATG groups were selected as candidates. The selected lncRNAs promoter were obtained from the Genome Browser or Eukaryotic Promoter Database.

Validation phase (III) consists of two steps: a) the lncRNA levels in breast cancer and normal MCF7 cell lines before and after exposure to ZnO-NPs was analyzed via real-time polymerase chain reaction (RT-PCR), b), the methylation status of lncRNA promoters and CpG island were investigated via MeDIP-RT-PCR and chromatin immunoprecipitation (ChIP).

Cell culture and treatment with ZnO-NPs

MCF-7 cells were obtained from the National Cell Bank of Iran (Pasteur Institute of Iran). MCF-7 cells were cultured in DMEM supplemented containing horse serum (5%), EGF (100 mg/mL), hydrocortisone (0.5 mg/ml), insulin (10 mg/mL) and 1% penicillin-streptomycin. Cells were grown under conditions of 5% CO_2 and 37 ˚C in a controlled humidified incubator. ZnO-NPs stock solution (2 mg) was suspended in 800 µL of distilled water and sonicated in an ice-water bath for 30 min at 30 W. Immediately, after sonication, 100 µL of BSA (15%) and 100 µL of PBS (10X) added to 800 µL distilled water of suspension. The dilutions of ZnO-NPs were vigorously vortexed for 30 s before cell exposure to avoid NPs agglomeration. The cell exposed to ZnO-NPs were done when the cells had grown to about 80% confluence.

Cytotoxicity assay

The cell viability of the MCF-7 cells after treatment with ZnO-NPs was tested by 3-(4,5-dimethylthiazol-2-yl)-2,5-diphenyltetrazolium bromide (MTT) assay. To evaluate the proliferative activity, MCF-7 counted and added to 4×10^4 cells per mL each well and exposed to various concentrations (range 1–100 µg/mL) and then incubated for 24-72 h. Wells containing medium but no cells were used as the blank, and wells containing culture medium without ZnO-NPs treatment were used as the control. The amount of 20 µL of MTT solution at 5 (mg/mL) was added to each well and incubated for 4 h at 37 ˚C. The MTT medium was discarded and the cells were lysed in 100 µL of DMSO. Afterwards, 60 µL of the DMSO was added to each well and incubated in room temperature (RT) for 30 min. The resulting Formosan crystals were solubilized and quantified by measuring absorbance at 570 nm by a multiwell-plate reader (Flex station III, Molecular Devices, Sunnyvale, CA, USA).

The viability was calculated as the ratio of exposure cell absorbance to control cell absorbance (OD ZnO-NPs−OD blank)/(OD control – OD blank)×100%). This experiment was carried out in triplicate. The DMSO (0.1%) was used as negative control.

Colony-forming assay

A colony-forming assay is used to determine the cells' re-proliferation capacity and disseminated tumor cells after treatment with NPs. The breast cancer cells (50 cells/well) were seeded into a 96-well plate and incubated for 24 h. The MCF-7 cells were treated to concentrations ranging from 1-100 µg/mL for 10 days in the CO_2 incubator. Cells were stained with 1% crystal violet (w/v) in 10% ethanol for 30 min. Percent viability was calculated by dividing the number of colonies formed by the number of cells plated per 100.

Determination of cytochrome c

In the intrinsic apoptotic pathway, cytochrome c (Cyt c) release from mitochondria was the main marker inactivates cell death. The concentrations of Cyt c (Cat. No. RBMS263R) in cell apoptosis were determined by using a sandwich enzyme-linked immunosorbent assay (ELISA) kit (BioVender Laboratory Medicine, Inc., Czech Republic). Antibody specific for human Cyt c (1 µg/mL) was coated onto a microplate well. Standards, samples, and controls were added into designated microplate wells and specific biotin-conjugated antibody was also pipetted to all wells and incubated at 37 ˚C for 120 min. After washing the plates 3 times with 1× PBST (phosphate-buffered saline with Tween 20), streptavidin-HRP was added into each well and incubated at room temperature for 1 h. In the next wash step, TMB substrate was added to the microplate wells. The reaction was terminated by addition of 20 µL of sulfuric acid solution (1 M) and absorbance was measured at the wavelength of 450 nm using the microplate reader. The experiment was repeated three times in triplicate wells.

ROS

Intracellular mitochondrial ROS were measured by 2′, 7′-dichlorodihydrofluorescein diacetate (Sigma-Aldrich Co.). after cell-treated with ZnO-NPs 10-100 µg/mL for 24-48 h, cells washed with PBS and then cells were incubated at 37 ˚C with 2′,7′- dichlorodihydrofluorescein diacetate for 20 minutes. The amount of fluorescence was determined using excitation at 485 nm and emission at 530 nm. Fluorescence intensity is related to the amount of ROS formed intracellularly.

Apoptosis detected by flow cytometry

Cells were made into 1×10^6/mL suspension after being digested with 0.25% trypsin, cleaned twice with PBS, mixed with 100 µL binding buffer, etc. After that, 10 µL of Annexin V-FITC and 10 µL of propidium iodide (PI) were

supplemented to the suspension. The suspension was incubated 5 min at room temperature in the dark and detected by NovBCyte flow cytometry (Derica Biotechnology Co., Ltd., Beijing, China, DLK0002051). The test was repeated 3 times and results were averaged.

Analysis of genomic DNA methylation

DNA genomic was extracted using THPG methods according to the method described previously. The percentages of DNA methylation levels were calculated by a MethylFlash Methylated DNA Quantification Kit, an ELISA-based colorimetric assay (Epigentek, Brooklyn, NY, USA) according to the manufacturer's instructions [31].

Total RNA extraction and RT-PCR

To study gene expression, MCF-7 cells were exposed to ZnO-NPs for 48 h. The control group contained MCF-7 cells with no NP exposure. Total RNA was extracted according to the manufacturer's instructions for RNA extraction kit (Zistabzar pajoohan, Iran) and spectrophotometrically assessed for its quality. cDNA was prepared using BioFact™ RT Series (Korea). To evaluate the expression of selected lncRNA, synthesized cDNAs were used for RT-PCR experiments. Genes were analyzed by SYBR Green fluorescence real-time RT-PCR with a Rotor-Gene Q instrument (Qiagen, Hilden, Germany). Primers stated in Table 1 were designed using AlleleID software version 7.5 (Premier Biosoft, USA). The RT-PCR reactions were used for RT-PCR according to the corresponding protocol (Takara, Japan). The RT-PCR reactions were set up in similar conditions Real-time qPCR. The relative expression of genes was calculated using the ($2^{-\Delta\Delta Ct}$) method and normalized using the *ACTB* as the internal control.

MeDIP-RT-PCR

According to the manufacturer's instructions, we used MeDIP kit (ab117133, Abcam, USA) for the analysis of methylation of the promoter and CpG island region of selected lncRNA along with enrichment and capture from the total methylation regions on genome DNA. Real-time qPCR was performed to evaluate the methylation status of promoter and CpG island region genes before and after ZnO-NPs treatment. The qPCR reactions were set up in a volume of 20 µL containing SYBR Green (RealQ plus Master Mix Green without ROX, Ampliqon, Denmark.) with GC buffer (Kawsar, Iran). The qPCR reactions were set up in a volume of 20 µL containing SYBR Green (RealQ plus Master Mix Green without ROX, Ampliqon, Denmark.) with GC buffer (Kawsar, Iran) Specific primers and methylated DNA. The amplification program consisted of an initial denaturation of 95 ˚C for 15 min, followed by 40 cycles of 95 ˚C for 15 s, 60 ˚C for 15 s, and 72 ˚C for 15 s. All sample reactions were performed in triplicates and the

Table 1. Primer pairs used to amplify specific methylated sequences

Gene	Location	Forward	Reverse	Size (bp)
PVT1	chr8:127793836-127794653	5′-AACTCGGCTTCTGGA-3′ 5′- CGAAGGAGGCGAGAAGGT-3′	5′-CACATCTTTGCTCGC-3′ 5′-TTTCCACGGTCTTTCC-3′	756 178
NORAD	chr20:36050328.36051042	5′- GACTTCGCTCACCTT-3′ 5′- CAATGGCGACAGAGTG-3′	5′- AACCTCTCTTTCCCAC-3′ 5′- GAAGTATGGCGGCAGC-3′	383 154
GAS5	chr1:173868035-173868779	5′- CCTCAATCTTCCTCT-3′ 5′- CATCCAGTATCACCTTCTTCC-3′	5′-GTATCTGGGTGTGTC-3′ 5′- CTCTTCCTCCTCAGTCGG-3′	586 131
CASC15	chr6:21666209-21666631	5′- GCAGAGTTGTGATGA-3′ 5′- TGAGAGGGAGAAACC-3′	5′- CAGCAGAGAAAGTCG-3′ 5′- CGAGAGGGAGATACC-3′	278 126
ZFAS1	chr20:49278022-49278662	5′- GGCGGGAGATGACTG-3′ 5′- GCCTGGACAACTACTA-3′	5′- GCGAAAGAACGAATGG-3′ 5′- GCGAAAGAACGAATGG-3′	328 167
TUG1	chr22:30968579-30969589	5′- AGATGGTGACAGGATT-3′ 5′- TCACAGACACCACAGC-3′	5′- TACGAGAAGAAAGACG-3′ 5′- AAAGCAGGAAGAGAGG-3′	627 250
DANCR	chr4:52712192-52713071	5′- GGGCACCGTAACAAT-3′ 5′- GGGCACCGTAACAAT-3′	5′- TGGCGACAAACAGAC-3′ 5′- GCTAAGAACTGAGGCA-3′	270 167
XIST	chrX:73850959-73851949	5′- GCAGCAATCCAGCA-3′ 5′- GCACTGTCCATCC-3′	5′- TGTCGCAGTGTTCAAGT-3′ 5′-CTCGGCTGAAGGTCT-3′	339 225
HOTAIR	chr12:53973032-53975319	5′- TTGGGTCAGTCCGATT-3′ 5′- TTTGGGTCAGTCCGATT-3′	5′- CAGAGTTGCTTGGGTTT-3′ 5′- GCTCCTCTAAGTTCACGAT-3′	495 244
MALAT1	chr11:65497487-65497927	5′- TCACAAAGGGAGGG-3′ 5′- CGGCGTTTGTCCCT-3′	5′- GAGGCGTCAGAGG-3′ 5′- GCTTCTGCGTTGCTAA-3′	280 160
ACTB	chr7:5529432-5530963	5′- GCGTTATTACCATA-3′ 5′-CGCACGCTGATTGG -3′	5′-CTCTTCCTCAATCT-3′ 5′-CCTCCTCCTCTTCCTC -3′	169 129

Human reference genome (hg38).

mean of the three reactions was considered as a representative value for each sample. Melting curve analysis was carried out following each reaction to verify the specificity of the products and the absence of primer dimers.

Preparation of standard curve

The standard curves were established using serially diluted concentrations of the selected lncRNA for an absolute quantification according to the method as described [31]. Thus, the nested PCR reaction was performed to amplify the selected regions using 4 specific primer sets. Both PCR reaction solution contained 5 µL DNA, 12.5 µL Taq DNA polymerase master mix RED (Ampliqon, Denmark), 10 pM of each primer, GC buffer and ddH_2O per 25 µL total reaction volume. Each PCR reaction was carried out using a thermal cycler gradient PCR system (Eppendorf, Germany). The first amplification program included predenaturation at 95 ˚C for 10 min, followed by 40 cycles of 94 ˚C for 30 s, 57 ˚C for 30 s, 72 ˚C for 1 min and final extension 72 ˚C for 10 min; and the second amplification program were predenaturation at 95 ˚C for 10 min, followed by 40 cycles of 94 ˚C for 30 s, 60 ˚C for 30 s, 72 ˚C for 1 min and final extension 72 ˚C for 10 min. The concentration of selected lncRNA in the stock solution was analyzed using a fluorospectrometric technique. The Finnzymes program was used to calculate the initial copy number of the calibrator dilution in the standard series. The standard series of 6.6 pg was used to convert the copy number to genome equivalents (GEq).

ChIP assay

Histone modification includes cytosine methylation and histone tail methylation which regulate chromatin structure, function and gene expression [32]. Epigenetic marks induced by ZnO-NPs on histone modification in promoter and CpG island of selected lncRNA genes were quantified with ChIP assay, followed by RT-PCR. To perform ChIP assays, exposed and not-exposed MCF-7 cells were lysed. Subsequently, cross-linked chromatin was sonicated and incubated with 3 µg antibody against H3K4me3 (Abcam: ab1012, broadly distributed on active enhancers and transcription start site (TSS)) and H3K27me3 (enriched around inactive transcription start site (TSS)) (Abcam, USA) at 4 ˚C overnight. The immune-complex was precipitated with protein A-agarose (Upstate, Charlottesville, VA), and the obtained beads were washed and proteins were removed with 75 µg of proteinase K (45 ˚C for 4 h). The complex was incubated at 65 ˚C overnight, and then DNA was recovered by triton/heat/phenol/glycogen (THPG) extractions [31], and DNA dissolved in 50 µL of TE buffer. The RT-PCR assays were performed by employing the primers in Table 1.

Statistical analysis

Data analysis of qPCR was performed with Prism, version 9.0.0 (GraphPad Software, Inc., La Jolla, CA, USA). Data were expressed as Mean±SD, and statistical significance was tested among and between groups using one-way and 2-way ANOVA, respectively, followed by post hoc Tukey's multiple-comparison or Bonferroni tests when appropriated. Differences with $P<0.001$ were considered to be statistically significant. All experiments were done at least three times unless otherwise indicated.

Results

Characterization of ZnO-NPs

The synthesized ZnO-NP in this study was characterized by a variety of techniques and the results were reported in this section. Transmission electron microscopy (TEM) (Figure 1) shows homogenous hexanol shape ZnO-NPs as

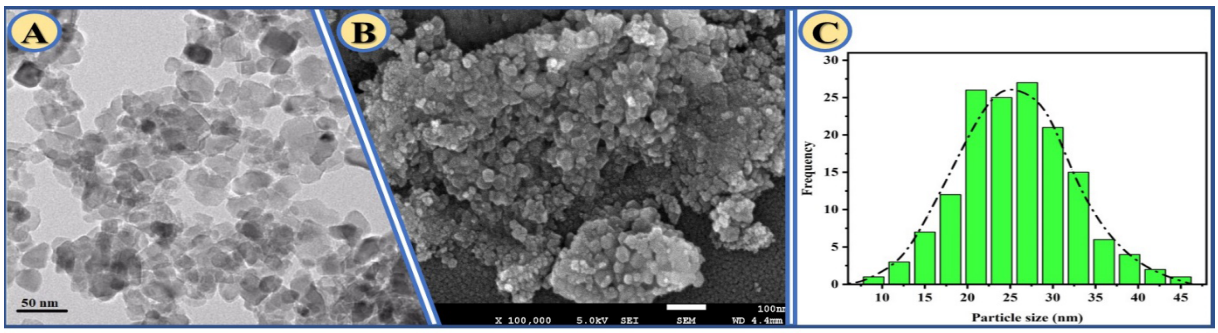

Figure 1. Characterization of ZnO-NPs

A) SEM image showing the surface morphology and overall structural features of ZnO-NPs, B) TEM image demonstrating the size, shape, and dispersion of the nanoparticles at higher resolution. © Particle size distribution analysis indicating the average diameter and size range of the synthesized ZnO-NPs.

a piece of evidence for the good quality of the NPs. Furthermore, the scanning electron microscope (SEM) micrograph (Figure 1) is used to study the physical characterization and morphological structure of NPs and confirm the homogenous shape and structure of synthesized ZnO-NPs. The size histogram of synthesized ZnO-NPs (presented in (Figure 1) indicates that the average size of NPs is about 25±6 nm.

The UV-vis absorption spectra of dispersed ZnO-NPs in ethanol 30% (0.1% v/w) is presented in Supplementary Figure 2. The ZnO-NPs characteristic absorption peak at wavelength 357 nm is highlighted accordingly [33]. The sharp peak indicates that the particle size is narrow. The XRD pattern of synthesized ZnO-NPs is presented in Supplementary Figure 2 and all highlighted peaks indexed to ZnO-NPs structure. Figure 2 shows high purity of NPs with intense, narrow and diffraction peaks. Brunauer-Emmett-Teller (BET) test was carried out by N2 adsorption temperature of 77k.

Figure 2C represents the nitrogen (N_2) adsorption-desorption isotherms of ZnO-NP from BET study. It is a relatively flat typical type 4 adsorption similar to the results obtained by Zhou et al. [34]. This finding confirms that the mean particle size obtained from BET agrees with TEM and XRD particle size finding (25±6 nm). Fourier Transform Infrared (FTIR) spectroscopy was performed to analyses and determine the active functional group of solvothermal method synthesized ZnO-NPs (Figure 2). A broad absorption band at 370 cm^{-1} attributes to Zn-O stretching vibration and correspond to E2 mode of hexagonal ZnO. Furthermore, other small absorption band at 930, 1050, and 3400 cm^{-1} are determined. These absorption band were corresponded to symmetric O-C-O and O-H stretching vibration of adsorbed CO_2 and H_2O from the air which can be abandoned. These results indicate the high purity of synthesized ZnO-NPs.

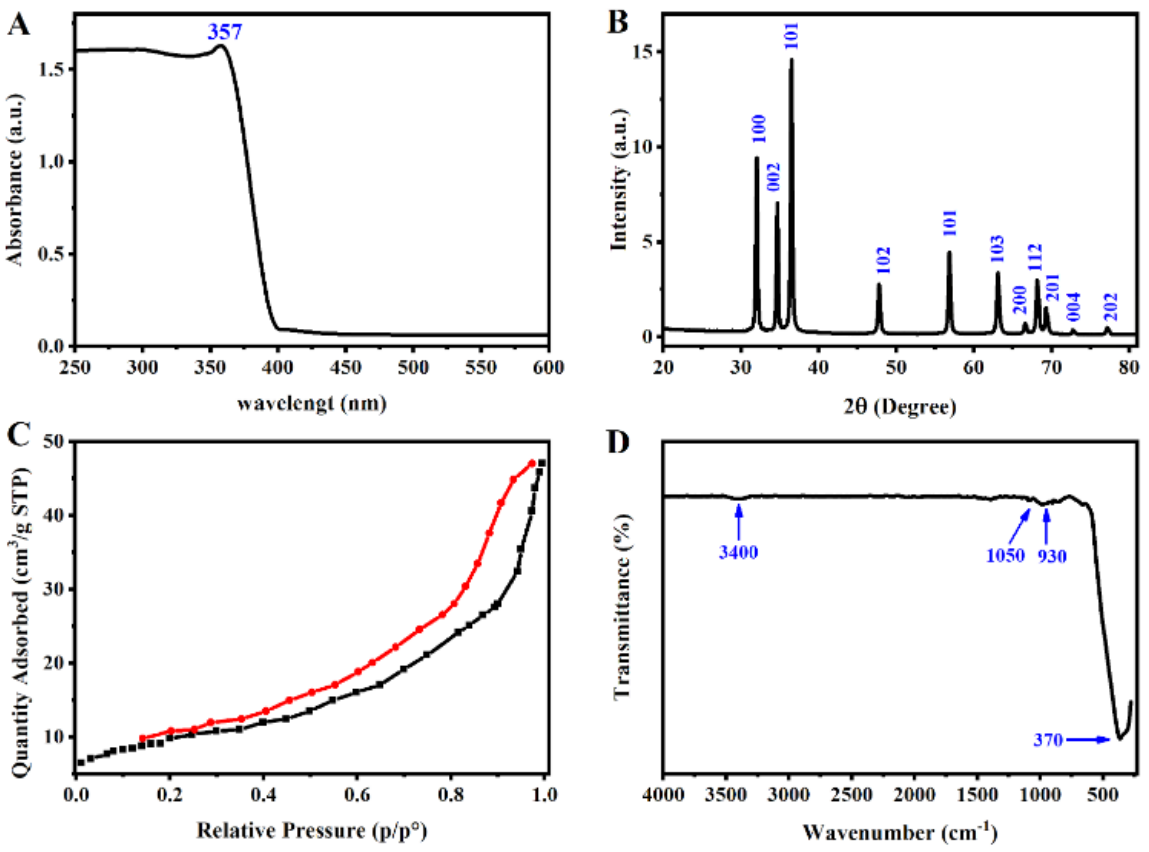

Figure 2. Physicochemical characterization of synthesized ZnO-NPs

A) UV–vis absorption spectrum of dispersed ZnO-NPs, B) X-ray diffraction (XRD) pattern of synthesized ZnO-NPs confirming their crystalline structure, C) Nitrogen adsorption–desorption isotherms of ZnO-NPs obtained from the BET analysis., D) FTIR spectrum used to identify the functional groups present on the surface of solvothermally synthesized ZnO-NPs

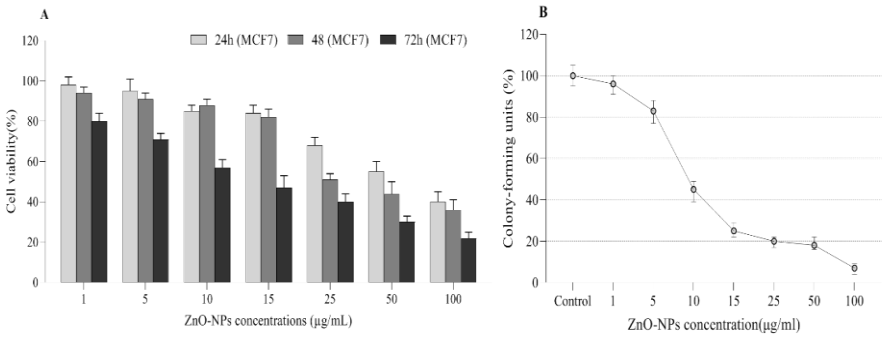

Figure 3. Effects of ZnO nanoparticles on the viability and proliferative capacity of MCF-7 breast cancer cells

A) Cell viability assessed by MTT assay following treatment of MCF-7 cells with different concentrations of ZnO-NPs (1–100 µg/mL) for 24, 48, and 72 h, B) Colony-forming assay showing the long-term proliferative ability of MCF-7 cells exposed to varying concentrations of ZnO-NPs for 10 days, with visual representation of colony formation and corresponding cell viability percentages.

Note: Data are presented as Mean±SE from at least three independent experimen.

Cytotoxicity of ZnO NPs

To evaluate the viability of MCF-7 cells following exposure to ZnO-NPs (1–100 µg/mL), an MTT assay was performed after 24, 48, and 72 h of treatment. The results demonstrated a significant dose- and time-dependent cytotoxic effect. Increasing concentrations of ZnO-NPs and longer exposure times markedly reduced cell viability. Based on these findings, 15 µg/mL at 48 h was selected for subsequent experiments, as this condition induced moderate cytotoxicity without causing excessive cell death that could obscure subtle epigenetic alterations (Figure 3A).

The long-term proliferative capacity of treated cells was further assessed using a colony-forming assay (Figure 3B). ZnO-NP exposure significantly reduced colony formation in a concentration-dependent manner, indicating effective inhibition of cell proliferation in MCF-7 cells

Determination of Cyt c

Cyt c release from mitochondria is a key event in the intrinsic apoptotic pathway. In this study, the level of Cyt c significantly increased following treatment with ZnO-NPs in both a dose- and time-dependent manner (Figure 4A). The highest Cyt c release was observed after exposure to

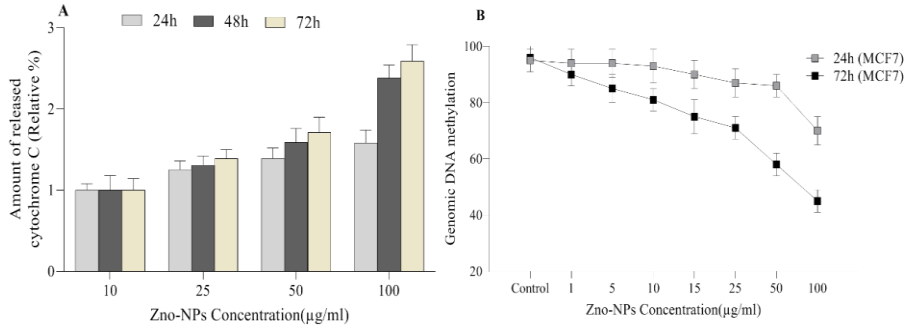

Figure 4. Effects of ZnO nanoparticles on mitochondrial apoptosis signaling and global DNA methylation in MCF-7 cells

A) Release of cytochrome c into the cytosol of MCF-7 cells following treatment with ZnO-NPs (10, 25, 50, and 100 µg/mL) for 24–72 h, indicating activation of the mitochondrial apoptotic pathway, B) Global genomic DNA methylation levels in MCF-7 cells after exposure to different concentrations of ZnO-NPs (1–100 µg/mL) for 24 and 72 h, demonstrating dose-dependent alterations in DNA methylation status

Note: Data are presented with a Mean±SE of at least three independent experiments.

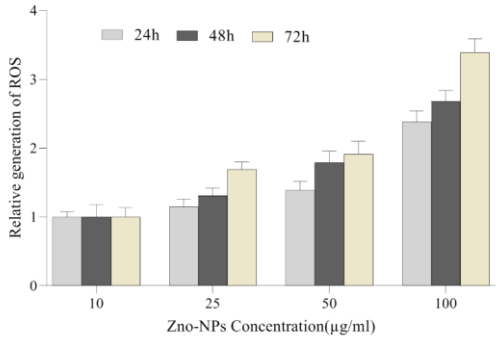

Figure 5. ROS generation in MCF-7 cells treated with ZnO-NPs

Note: Relative fluorescence intensity of sample versus control was calculated. Data are presented as mean± standard deviation (n=3 wells/treatment).

100 μg/mL ZnO-NPs for 72 h compared with the control group. These findings indicate that ZnO-NP treatment promotes mitochondrial membrane disruption and triggers the mitochondrial apoptotic pathway. Consistently, MCF-7 breast cancer cells exposed to increasing concentrations of ZnO-NPs exhibited progressively higher Cyt c release over time, further supporting the role of ZnO-NPs in inducing apoptosis through mitochondrial signaling.

ZnO-NP exposure on genomic DNA methylation

Global genomic DNA methylation levels in MCF-7 cells were evaluated after exposure to different concentrations of ZnO-NPs (1, 5, 10, 15, 25, 50, and 100 μg/mL) for 24 and 72 h (Figure 4B). The results demonstrated that ZnO-NP treatment significantly altered the genomic DNA methylation profile. A clear dose-dependent

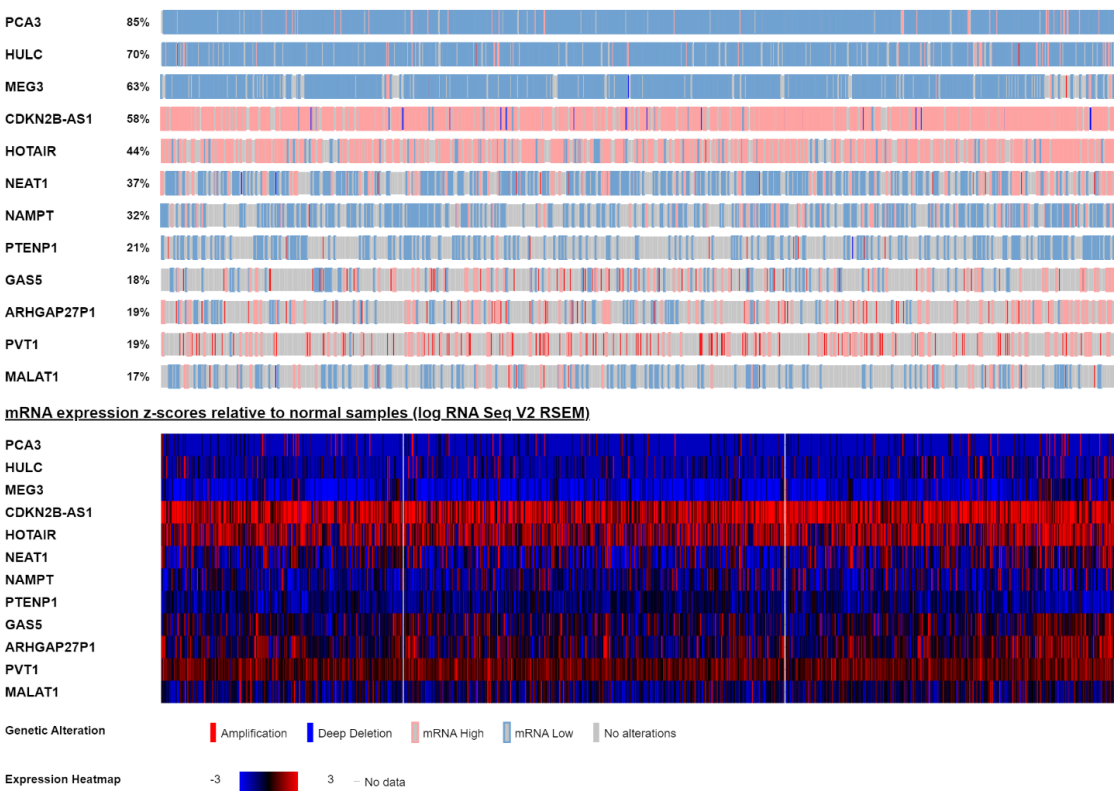

Figure 6. Identification of differentially expressed lncRNAs in breast cancer using TCGA data

Note: Heatmap representing the expression profiles of the top 10 selected lncRNAs in breast cancer samples retrieved from the TCGA database via cBioPortal. These lncRNAs include PVT1, NORAD, GAS5, CASC15, ZFAS1, TUG1, DANCR, XIST, HOTAIR, and MALAT1. The heatmap illustrates the differential expression patterns of these candidate lncRNAs across breast cancer samples.

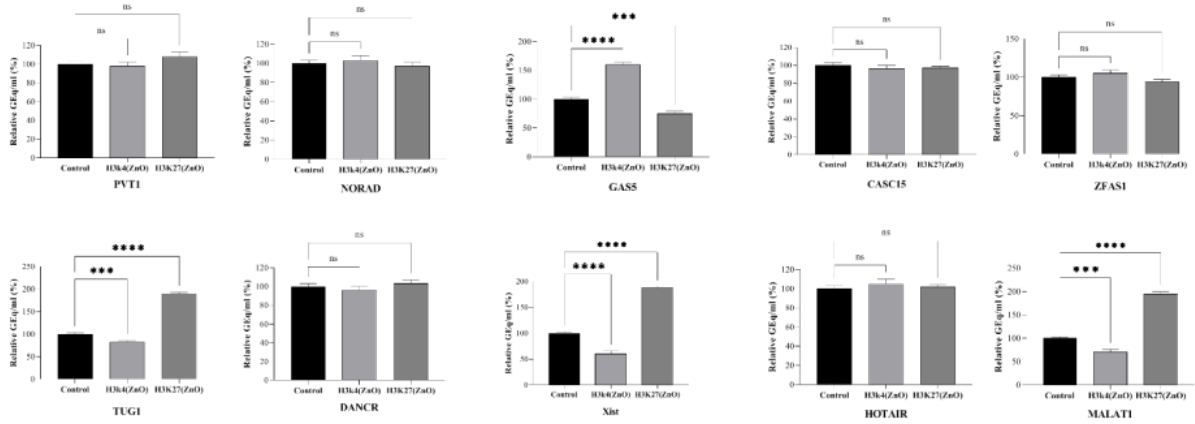

Figure 7. Effects of ZnO-NP exposure on the expression of autophagy- and cancer-related lncRNAs in MCF-7 cells

Note: Relative expression levels of *PVT1*, *NORAD*, *GAS5*, *CASC15*, *ZFAS1*, *TUG1*, *DANCR*, *XIST*, *HOTAIR*, and *MALAT1* in MCF-7 breast cancer cells following exposure to 15 µg/mL ZnO nanoparticles (ZnO-NPs) for 48 h. Gene expression was quantified by qRT-PCR and normalized to the internal control gene. Results represent the Mean±SD of three independent experiments (n=3). Error bars indicate the standard deviation among replicates

decrease in DNA methylation levels was observed compared with the untreated control cells. The methylation percentage progressively declined from approximately 85% in control cells to about 42% in cells treated with higher concentrations of ZnO-NPs. These findings indicate that exposure to ZnO-NPs induces global DNA hypomethylation in MCF-7 cells, suggesting that ZnO-NPs may influence epigenetic regulation in breast cancer cells

ZnO-NPs induced production of ROS in MCF-7

ROS generation in MCF-7 cells treated with ZnO-NPs increased in a dose- and time-dependent manner. The highest level of ROS production was observed after treatment with 100 µg/mL ZnO-NPs for 72 h, which was significantly greater than that observed at lower concentrations and shorter exposure times. A marked increase in fluorescence intensity was also detected after treatment with 25 µg/mL for 48 h compared with the control group. In contrast, the increase in ROS at lower concentrations such as 5–10 µg/mL was relatively modest (Figure 5).

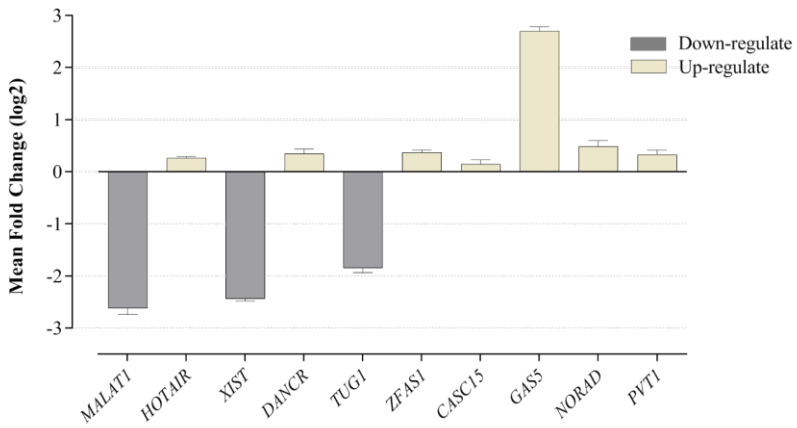

Figure 8. Fold change in the expression of the top 10 lncRNAs in MCF-7 cells following exposure to ZnO-NPs

Note: Relative expression levels of *PVT1*, *NORAD*, *GAS5*, *CASC15*, *ZFAS1*, *TUG1*, *DANCR*, *XIST*, *HOTAIR*, and *MALAT1* were quantified by qRT-PCR after treatment of MCF-7 cells with ZnO-NPs. Gene expression was normalized to the internal control gene ACTB, and fold changes were calculated relative to untreated control cells. Data are presented as Mean±SE from three independent biological replicates. Statistical significance was determined compared with the control group.

Screening of BC-associated candidate lncRNA

To investigate the effect of ZnO-NPs on lncRNA expression in breast cancer, the top 10 differentially expressed lncRNAs were selected from the TCGA cBioPortal database. These lncRNAs included PVT1, NORAD, GAS5, CASC15, ZFAS1, TUG1, DANCR, XIST, HOTAIR, and MALAT1, and were used as candidate targets for further analysis in this study (Figure 6).

MeDIP- RT-PCR

The methylation status of promoter and CpG island selected lncRNAs was evaluated by MeDIP-real time quantitative PCR (primers in Table 1) in MCF-7 cells after exposure with ZnO-NPs. The results for the analysis lncRNAs are shown in Table 2. After exposed with ZnO-NPS, the promoter methylation patterns showed that the lncRNA including GAS5 exhibited significantly decreased methylation in their promoters. Also, our result showed that MALAT1, TUG1, and XIST exhibited significantly increased methylation in their promoters. However, PVT1, DANCR, CASC15, HOTAIR, NORAD, and ZFAS do not show a significant alteration in methylation status.

Histones modification analysis

H3K27me3 and H3K4me3 histone modification marks at the promoter and CpG island regions of selected lncRNAs were evaluated to investigate histone tail modification status following ZnO-NP exposure in MCF-7 cells. As shown in Figure 7, ZnO-NP treatment significantly decreased H3K27me3 levels while increasing

Table 2. The promoter methylation patterns before and after ZnO-NP exposure

Treatment Condition	No.	LncRNAs	Mean Ct	Mean Genomic Equivalent (GEq/mL)	StDev Genomic Equivalent
Before Exposure with ZnO-NPs	1	PVT1	28.14	172.81±6.02	[157.85, 187.76]
	2	NORAD	28.39	145.41±7.9	[125.78, 165.03]
	3	GAS5	28.3	155.42±5.65	[137.50, 165.33]
	4	CASC15	30.19	42.53±1.66	[38.40, 46.65]
	5	ZFAS1	28.06	182.96±6.9	[165.81, 200.1]
	6	TUG1	29.34	76.06±2.85	[68.98, 83.13]
	7	DANCR	29.42	71.89±2.46	[65.77, 78.00]
	8	XIST	29.19	84.37±5.76	[70.06, 98.67]
	9	HOTAIR	29.46	70.24±2.56	[63.88, 76.59]
	10	MALAT1	28.66	121.64±5.75	[107.35, 135.92]
After Exposure with ZnO-NPs	1	PVT1	28.23	149.64±9.8	[125.02, 174]
	2	NORAD	28.69	118.47±7.4	[100.09, 136.86]
	3	GAS5	30.26	33.14±2.31	[27.40, 38.87]
	4	CASC15	30.56	43.31±1.67	[39.16, 47.45]
	5	ZFAS1	28.53	132.47±8.2	[112.1, 152.83]
	6	TUG1	28.51	134.24±6.87	[117.17, 151.30]
	7	DANCR	29.17	85.62±2.69	[78.93, 92.30]
	8	XIST	28.32	152.81±6.06	[137.75, 167.86]
	9	HOTAIR	29.03	93.81±3.49	[85.14, 102.47]
	10	MALAT1	27.27	314.5±26.8	[247.92, 381.07]

H3K4me3 enrichment at the GAS5 locus. In contrast, MALAT1, XIST, and TUG1 exhibited a significant increase in the repressive H3K27me3 mark accompanied by a decrease in the activating H3K4me3 mark. However, no significant changes in either H3K4me3 or H3K27me3 enrichment were observed at the promoter or CpG island regions of *PVT1*, *DANCR*, *CASC15*, *HOTAIR*, *NORAD*, or *ZFAS1*. These findings indicate that ZnO-NP exposure modulates the epigenetic landscape of specific lncRNAs by altering activating and repressive histone marks, which may contribute to the regulation of their transcriptional activity.

Gene expression analysis

Relative expression levels of the selected lncRNAs were evaluated in control and ZnO-NP–treated MCF-7 cells (15 µg/mL, 48 h) using qRT-PCR (Figure 8). Expression values were normalized to ACTB and calculated relative to untreated control cells. ZnO-NP exposure resulted in a significant upregulation of GAS5. In contrast, MALAT1, XIST, and TUG1 were significantly downregulated following treatment. Although *PVT1*, *DANCR*, *CASC15*, *HOTAIR*, *NORAD*, and *ZFAS1* exhibited a slight increase in expression, these changes were not statistically significant compared with the control group. Data are presented as Mean±SE from three independent biological replicates.

Discussion

Human exposure to NPs including engineered and natural ones may happen in different ways throughout the lifetime. Thus, a range of associated adverse effects on human health may be expected from NPs side. The toxicity of NPs is commonly generated by the generation of free radicals and oxidative stress [35]. Previous studies showed that NPs toxicity depends on their dose and exposure time [36]. Therefore, synthesized NPs have been proposed for epigenetic therapy. The major observed effect of ZnO-NPs exposure is reduced the level of global DNA methylation [37]. The most important epigenetic modification, including DNA methylation patterns, histone modification, and ncRNA profiles. However, the effect of ZnO-NP on epigenetics, including ncRNA expression is not been investigated. This work represents the first study to investigate the effect of nanoparticle-induced epigenetic effects on breast cancer MCF-7 cells and to evaluate this effect on ROS-regulator lncRNA.

Treatment with ZnO-NPs was found to reduce not only the amount of genomic DNA methylation, but also the cell viability in breast cancer cell. In our study, we observed increase in genomic DNA hypomethylation (Figure 4) and ROS level (Figure 5) along with corresponding alteration in lncRNA expression at the 15 µg/ml of ZnO-NPs for 48 h (Figure 8). We compared 10 top lncRNA in treated and untreated conditions. Our study was based on quantitative analysis of lncRNA expression (quantitative real time PCR) and determination of promoter status of selected lncRNA using MeDIP-real time and ChIP assay. After exposure of MCF-7 to ZnO-NPs, we investigated whether changes in the expression of lncRNA could correlate with changes in promoter methylation and histone modification. The result reveal that the exposure to ZnO-NPs resulted in 4 lncRNA (GAS5, TUG1, XIST, and MALAT1) with significant altered expression levels in MCF-7 cells (Figure 8). Expression of MALAT1, XIST, and TUG1 were decreased at 15 µg/mL for ZnO-NPs at 48 h. In contrast, TUG1 expression significantly increased under the same conditions. Also, the results of DNA methylation and histones modification were consistent with the lncRNA expression profiles. It seems that increased cell death and ROS level in ZnO-NPs exposed cells are associated with more epigenetic alterations of lncRNA involved in the regulation of intracellular ROS.

Several studies showed that ZnO-treat of cancer cells increase cellular ROS and cell death [38-40]. Also, the recently studies reveal that lncRNA acts as major regulators of cell stress in cancer [29, 41]. In this study, we have hypothesized that crosstalk between ZnO-NPs and ROS leads to altered epigenetic of lncRNA, which regulate ROS generation and removal. The results indicate a significant relationship between ROS production and changes in the expression of ROS regulator lncRNA.

Metastasis-associated lung adenocarcinoma transcript 1 (MALAT1) located at 11q13, also known as (NEAT2) with a size of about 8 kb, is highly conserve and abundant lncRNAs in normal mamalian tissues. Knockdown of MALAT1 suppressed proliferation, motility, and increased apoptosis in vitro [42].

Conclusion

Previous studies have reported that global DNA hypomethylation leads to overexpression of genes that is important in carcinogenesis. However, in this study, we hypothesized that increased global DNA hypomethylation that was associated with ZnO-NPs leads to regulated lncRNA expression involve in regulation ROS generation. In conclusion, our data suggest strong correlation between ZnO-NPs exposure, lncRNA (ZFAS1, MALAT1, and PVT1) expression, and amount of vi-

ability and apoptosis in MCF7 cells. The present study provides new insights into the mechanism of genotoxic effects and epigenetic of ZnO-NPs on lncRNA profile in breast cancer cells. It is important to assay the toxicity of NPs before use of them in medicine. To our knowledge, this is the first report on genetic and epigenetic study of ZNO-NPs effect on lncRNA expression in breast cancer. Further researches are needed to fully characterize the relation between observed including the alteration in lncRNA expression and the effect of ZnO-NPs observed at the cellular level.

Ethical Considerations

Compliance with ethical guidelines

There were no ethical considerations to be considered in this research.

Funding

This research did not receive any grant from funding agencies in the public, commercial, or non-profit sectors.

Authors' contributions

Conceptualization: Ali Saberian and Mostafa Akbariqomi; Funding acquisition: Mostafa Akbariqomi and Sara Keshtkari; Resources: Mostafa Akbariqomi and Sara Keshtkari; Software: Reza Heidari; Validation: Mostafa Akbariqomi and Reza Heidari; Formal analysis: Reza Heidari and Sara Keshtkari; Data curation: Ali Saberian and Reza Heidari; Visualization: Sara Keshtkari and Reza Heidari; Writing the original draft: Ali Saberian; Methodology, investigation, review, editing and final approval: All authors; Supervision and project administration: Mostafa Akbariqomi.

Conflict of interest

The authors declared no conflict of interest.

Acknowledgments

The authors would like to express their sincere gratitude to the Comprehensive Laboratory of AJA University of Medical Sciences for providing the laboratory facilities and technical support required to conduct this study.

References

[1] Wiesmann N, Tremel W, Brieger J. Zinc oxide nanoparticles for therapeutic purposes in cancer medicine. Journal of Materials Chemistry. B. 2020; 8(23):4973-89. [DOI:10.1039/d0tb00739k] [PMID]

[2] Jiang J, Pi J, Cai J. The advancing of zinc oxide nanoparticles for biomedical applications. Bioinorganic Chemistry and Applications. 2018; 2018:1062562. [DOI:10.1155/2018/1062562] [PMID]

[3] Ahmed B, Dwivedi S, Abdin MZ, Azam A, Al-Shaeri M, Khan MS, et al. Mitochondrial and chromosomal damage induced by oxidative stress in Zn2+ Ions, ZnO-Bulk and ZnO-NPs treated Allium cepa roots. Scientific Reports. 2017; 7:40685. [DOI:10.1038/srep40685] [PMID]

[4] Durnev AD. Toxicology of nanoparticles. Bulletin of Experimental Biology and Medicine. 2008; 145(1):72-4. [DOI:10.1007/s10517-008-0005-x] [PMID]

[5] Gedda MR, Babele PK, Zahra K, Madhukar P. Epigenetic aspects of engineered nanomaterials: Is the collateral damage inevitable? Frontiers in Bioengineering and Biotechnology. 2019; 7:228. [DOI:10.3389/fbioe.2019.00228] [PMID]

[6] Bhattacharyya S, Kudgus RA, Bhattacharya R, Mukherjee P. Inorganic nanoparticles in cancer therapy. Pharmaceutical Research. 2011; 28(2):237-59. [DOI:10.1007/s11095-010-0318-0] [PMID]

[7] Cao D, Shu X, Zhu D, Liang S, Hasan M, Gong S. Lipid-coated ZnO nanoparticles synthesis, characterization and cytotoxicity studies in cancer cell. Nano Convergence. 2020; 7(1):14. [DOI:10.1186/s40580-020-00224-9] [PMID]

[8] Bisht G, Rayamajhi S. ZnO Nanoparticles: A promising anticancer agent. Nanobiomedicine (Rij). 2016; 3:9. [DOI:10.5772/63437] [PMID]

[9] Rasmussen JW, Martinez E, Louka P, Wingett DG. Zinc oxide nanoparticles for selective destruction of tumor cells and potential for drug delivery applications. Expert Opinion on Drug Delivery. 2010; 7(9):1063-77. [DOI:10.1517/17425247.2010.502560] [PMID]

[10] Dusinska M, Tulinska J, El Yamani N, Kuricova M, Liskova A, Rollerova E, et al. Immunotoxicity, genotoxicity and epigenetic toxicity of nanomaterials: New strategies for toxicity testing? Food and Chemical Toxicology. 2017; 109(Pt 1):797-811. [DOI:10.1016/j.fct.2017.08.030] [PMID]

[11] Zhang W, Zhao Y, Li F, Li L, Feng Y, Min L, et al. Zinc oxide nanoparticle caused plasma metabolomic perturbations correlate with hepatic steatosis. Frontiers in Pharmacology. 2018; 9:57. [DOI:10.3389/fphar.2018.00057] [PMID]

[12] Roberti A, Valdes AF, Torrecillas R, Fraga MF, Fernandez AF. Epigenetics in cancer therapy and nanomedicine. Clinical Epigenetics. 2019; 11(1):81. [DOI:10.1186/s13148-019-0675-4] [PMID]

[13] Ng CT, Yong LQ, Hande MP, Ong CN, Yu LE, Bay BH, et al. Zinc oxide nanoparticles exhibit cytotoxicity and genotoxicity through oxidative stress responses in human lung fibroblasts and Drosophila melanogaster. International Journal of Nanomedicine. 2017; 12:1621-37. [DOI:10.2147/ijn.s124403] [PMID]

[14] Yang D, Zhang M, Gan Y, Yang S, Wang J, Yu M, et al. Involvement of oxidative stress in ZnO NPs-induced apoptosis and autophagy of mouse GC-1 spg cells. Ecotoxicology and Environmental Safety. 2020; 202:110960. [DOI:10.1016/j.ecoenv.2020.110960] [PMID]

[15] Nunes T, Bernardazzi C, de Souza HS. Cell death and inflammatory bowel diseases: Apoptosis, necrosis, and autophagy in the intestinal epithelium. BioMed Research International. 2014; 2014:218493. [DOI:10.1155/2014/218493] [PMID]

[16] Chiarelli R, Martino C, Agnello M, Bosco L, Roccheri MC. Autophagy as a defense strategy against stress: Focus on Paracentrotus lividus sea urchin embryos exposed to cadmium. Cell Stress & Chaperones. 2016; 21(1):19-27. [DOI:10.1007/s12192-015-0639-3] [PMID]

[17] Zhang XH, Li BF, Ding J, Shi L, Ren HM, Liu K, et al. LncRNA DANCR-miR-758-3p-PAX6 molecular network regulates apoptosis and autophagy of breast cancer cells. Cancer Management and Research. 2020; 12:4073-84. [DOI:10.2147/cmar.s254069] [PMID]

[18] Lin YF, Chiu IJ, Cheng FY, Lee YH, Wang YJ, Hsu YH, et al. The role of hypoxia-inducible factor-1α in zinc oxide nanoparticle-induced nephrotoxicity in vitro and in vivo. Particle and Fibre Toxicology. 2016; 13(1):52. [DOI:10.1186/s12989-016-0163-3] [PMID]

[19] Johnson BM, Fraietta JA, Gracias DT, Hope JL, Stairiker CJ, Patel PR, et al. Acute exposure to ZnO nanoparticles induces autophagic immune cell death. Nanotoxicology. 2015; 9(6):737-48. [DOI:10.3109/17435390.2014.974709] [PMID]

[20] Shen J, Yang D, Zhou X, Wang Y, Tang S, Yin H, et al. Role of autophagy in zinc oxide nanoparticles-induced apoptosis of mouse LEYDIG cells. International Journal of Molecular Sciences. 2019; 20(16):4042. [DOI:10.3390/ijms20164042] [PMID]

[21] Yao H, Han B, Zhang Y, Shen L, Huang R. Non-coding rnas and autophagy. Advances in Experimental Medicine and Biology. 2019; 1206:199-220. [DOI:10.1007/978-981-15-0602-4_10] [PMID]

[22] Talebian S, Daghagh H, Yousefi B, □zkul Y, Ilkhani K, Seif F, et al. The role of epigenetics and non-coding RNAs in autophagy: A new perspective for thorough understanding. Mechanisms of Ageing and Development. 2020; 190:111309. [DOI:10.1016/j.mad.2020.111309] [PMID]

[23] Heidari R, Akbariqomi M, Asgari Y, Ebrahimi D, Alinejad-Rokny H. A systematic review of long non-coding RNAs with a potential role in breast cancer. Mutation Research. Reviews in Mutation Research. 2021; 87:108375. [DOI:10.1016/j.mrrev.2021.108375] [PMID]

[24] Zhu S, Wang J, He Y, Meng N, Yan GR. Peptides/proteins encoded by non-coding RNA: A novel resource bank for drug targets and biomarkers. Frontiers in Pharmacology. 2018; 9:1295. [DOI:10.3389/fphar.2018.01295] [PMID]

[25] Slack FJ, Chinnaiyan AM. The role of non-coding RNAs in oncology. Cell. 2019; 179(5):1033-55. [DOI:10.1016/j.cell.2019.10.017] [PMID]

[26] Lo PK, Wolfson B, Zhou Q. Cellular, physiological and pathological aspects of the long non-coding RNA NEAT1. Frontiers in Biology. 2016; 11(6):413-26. [DOI:10.1007/s11515-016-1433-z] [PMID]

[27] Liu L, Zhang Y, Lu J. The roles of long noncoding RNAs in breast cancer metastasis. Cell Death & Disease. 2020; 11(9):749. [DOI:10.1038/s41419-020-02954-4] [PMID]

[28] Zhang T, Hu H, Yan G, Wu T, Liu S, Chen W, et al. Long non-coding RNA and breast cancer. Technology in Cancer Research & Treatment. 2019; 18:1533033819843889. [DOI:10.1177/1533033819843889] [PMID]

[29] Connerty P, Lock RB, de Bock CE. Long non-coding rnas: major regulators of cell stress in cancer. Frontiers in Oncology. 2020; 10:285. [DOI:10.3389/fonc.2020.00285] [PMID]

[30] Shamhari MN, Wee SB, Chin FS, Kok YK. Synthesis and characterization of zinc oxide nanoparticles with small particle size distribution. Acta Chimica Slovenica. 2018; 65(3):578-85. [PMID]

[31] Akbariqomi M, Heidari R, Gargari SS, Omrani MD, Rigi G, Sanikhani NS, et al. Evaluation and statistical optimization of a method for methylated cell-free fetal DNA extraction from maternal plasma. Journal of Assisted Reproduction and Genetics. 2019; 36(5):1029-38. [DOI:10.1007/s10815-019-01425-w] [PMID]

[32] Figueroa ME, Reimers M, Thompson RF, Ye K, Li Y, Selzer RR, et al. An integrative genomic and epigenomic approach for the study of transcriptional regulation. PLoS One. 2008; 3(3):e1882. [DOI:10.1371/journal.pone.0001882] [PMID]

[33] Zak AK, Razali R, Majid WH, Darroudi M. Synthesis and characterization of a narrow size distribution of zinc oxide nanoparticles. International Journal of Nanomedicine. 2011; 6:1399-403. [DOI: 10.2147/IJN.S19693] [PMID]

[34] Zhou M, Wei Z, Qiao H, Zhu L, Yang H, Xia T. Particle size and pore structure characterization of silver nanoparticles prepared by confined arc plasma. Journal of Nanomaterials. 2009; 968058. [DOI: 10.1155/2009/968058]

[35] Ahamed M, Alsalhi MS, Siddiqui MK. Silver nanoparticle applications and human health. Clinica Chimica Acta; International Journal of Clinical Chemistry. 2010; 411(23-24):1841-8. [DOI:10.1016/j.cca.2010.08.016] [PMID]

[36] Jeng HA, Swanson J. Toxicity of metal oxide nanoparticles in mammalian cells. Journal of Environmental Science and Health. Part A, Toxic/Hazardous Substances & Environmental Engineering. 2006; 41(12):2699-711. [DOI:10.1080/10934520600966177] [PMID]

[37] Pogribna M, Hammons G. Epigenetic effects of nanomaterials and nanoparticles. Journal of Nanobiotechnology. 2021; 19(1):2. [DOI:10.1186/s12951-020-00740-0] [PMID]

[38] Wang C, Hu X, Gao Y, Ji Y. ZnO Nanoparticles treatment induces apoptosis by increasing intracellular ROS Levels in LTEP-a-2 cells. BioMed Research International. 2015; 2015:423287. [DOI:10.1155/2015/423287] [PMID]

[39] Guo D, Bi H, Liu B, Wu Q, Wang D, Cui Y. Reactive oxygen species-induced cytotoxic effects of zinc oxide nanoparticles in rat retinal ganglion cells. Toxicology in Vitro. 2013; 27(2):731-8. [DOI:10.1016/j.tiv.2012.12.001] [PMID]

[40] Choudhury SR, Ordaz J, Lo CL, Damayanti NP, Zhou F, Irudayaraj J. From the cover: zinc oxide nanoparticles-induced reactive oxygen species promotes multimodal cyto- and epigenetic toxicity. Toxicological Sciences. 2017; 156(1):261-74. [DOI:10.1093/toxsci/kfw252] [PMID]

[41] Wang X, Shen C, Zhu J, Shen G, Li Z, Dong J. Long non-coding rnas in the regulation of oxidative stress. Oxidative Medicine and Cellular Longevity. 2019; 2019:1318795. [DOI:10.1155/2019/1318795] [PMID]

[42] Miao Y, Fan R, Chen L, Qian H. Clinical Significance of long non-coding RNA MALAT1 expression in tissue and serum of breast cancer. Annals of Clinical and Laboratory Science. 2016; 46(4):418-24. [PMID]